Supramolecular Materials 1 (2022) 100002

Contents lists available at ScienceDirect

Supramolecular Materials

journal homepage: http://www.keaipublishing.com/en/journals/supramolecular-materials/

Stimuli-responsive hydrogel sponge for ultrafast responsive actuator

Yukun Jian[a,b,1], Baoyi Wu[a,b,1], Xuxu Yang[c], Yu Peng[a,b], Dachuan Zhang[a], Yang Yang[d], Huiyu Qiu[a], Huanhuan Lu[a,b], Jiawei Zhang[a,b,*], Tao Chen[a,b,*]

[a] Key Laboratory of Marine Materials and Related Technologies, Zhejiang Key Laboratory of Marine Materials and Protective Technologies, Ningbo Institute of Material Technology and Engineering, Chinese Academy of Sciences, Ningbo 315201, China
[b] School of Chemical Sciences, University of Chinese Academy of Sciences, 19A Yuquan Road, Beijing 100049, China
[c] Department of Engineering Mechanics and Center for X-Mechanics, Zhejiang University, Hangzhou 310027, China
[d] State Key Laboratory of Polymer Materials Engineering, College of Chemistry, Sichuan University, Chengdu 610064, China

ARTICLE INFO

Keywords:
Hydrogel sponge
Stimuli-response
Ultrafast
Actuator
Grabbing living creatures

ABSTRACT

With the ability to deform in response to specific stimuli, polymeric hydrogel actuators are important bionic materials. However, because shape deformation is derived from the diffusion of water molecules, the response rate of hydrogel actuators is usually slow, which severely limits their potential applications. In this work, a thermo-responsive PNIPAm hydrogel sponge is developed, and the hydrogel sponge shows ultrafast de-swelling/swelling capacity (equilibrium time 7 s) and large deformation degree (40%) due to the assistance of capillary force. Hydrogel sponge actuator with rapid response performance is further constructed, and the hydrogel sponge actuator could be used to capture moving objects and living creatures. Moreover, light-controlled directional movement can be achieved by incorporating photothermal functional components into the hydrogel sponge actuator. This work would promote the application of hydrogel actuators in soft robots.

1. Introduction

There are many fascinating biological activities in nature. Regardless of their size, they can move, grow and reproduce in different environments. Inspired by nature, researchers are committed to imitating the structure and function of animals or plants to design soft robots that are as flexible and reliable as living creatures.[1] Hydrogel, as a novel intelligent material similar in the structure of biological tissues, with diverse functions and strong compatibility, has been considered to be one of the best materials for designing soft intelligent robots.[2–6] Compared with other actuators such as liquid crystals and polymer films, hydrogel actuators could provide large deformation and better imitate the biology behavior of living organisms. Based on the stimuli-responsive property of hydrogels, and then using patterning and other methods to introduce anisotropic structure, researchers can construct hydrogel actuators that can respond to a variety of external stimuli (such as temperature, humidity, pH, ions, etc.), which can be used in soft robots, artificial muscles, intelligent controllers and other fields.[7–15]

Poly (*N*-isopropylacrylamid) (PNIPAm) hydrogel, as a typical thermal-induced shrinkage material, has been widely used to construct hydrogel actuators.[16–22] With a LCST of 32 °C, close to human body temperature, PNIPAm-based hydrogel actuators have promising potential in the fields of biomedical and soft robots. However, like other hydrogel-based actuators, the de-swelling or swelling of PNIPAm actuator depends on the diffusion of water molecules, and the actuating speed is usually low (deswelling > 1 min, swelling > 20 min),[16] which severely limits its practical applications, while humans and animals normally could complete the deformation action quickly (Fig. 1a). According to Fillmore's theory, the diffusion rate of water in hydrogel is inversely proportional to the square of the hydrogel's dimension.[23] However, though the microscopic hydrogel actuator possesses higher response speed, the application in macroscopic field is limited.

As known, the thermo-responsive deswelling property of PNIPAm is due to the transition from PNIPAm-water hydrogen bond to PNIPAm-PNIPAm hydrogen bond. Therefore, there are two major strategies to promote the swelling/deswelling rate: (1) Increasing the contact area of the aqueous solution and the hydrogel, [24-25] for instance, Agarwal et al. have synthesized porous PNIPAm-based bilayer membranes by electrospinning, and the PNIPAm polymer fibers greatly increase the specific surface area of the material, leading to the increasing of deformation speed.[25] (2) Increasing the size of pores in the hydrogel network, [26–29] which can help reducing the resistance encountered during mass transport, thereby increasing the diffusion rate of solvents. For example, Nie et al. have used pore-forming agent polyethylene glycol (PEG) to prepare composite hydrogel materials with large pores,

* Corresponding authors.
E-mail addresses: zhangjiawei@nimte.ac.cn (J. Zhang), tao.chen@nimte.ac.cn (T. Chen).
[1] These authors contributed equally to this work.

https://doi.org/10.1016/j.supmat.2021.100002
Received 11 August 2021; Received in revised form 7 October 2021; Accepted 8 October 2021

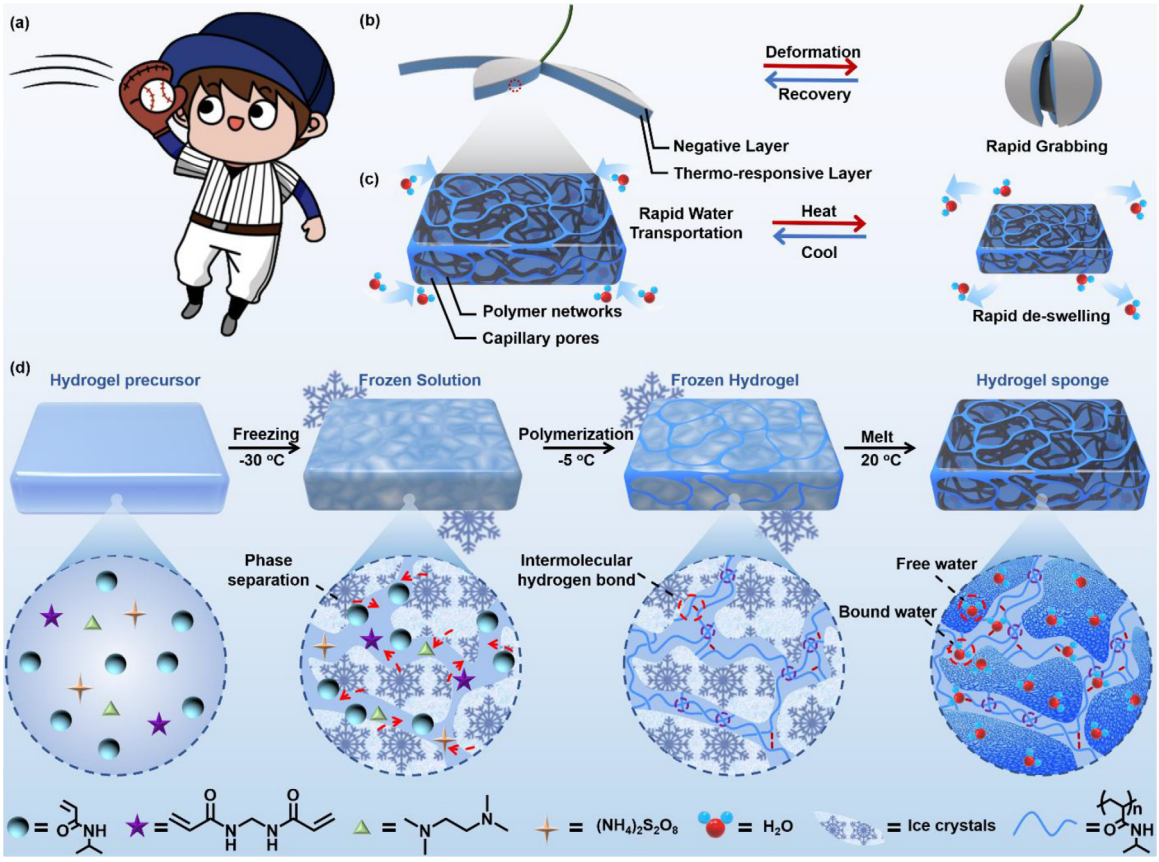

Fig. 1. (a) Schematic of a boy being able to grasp a moving ball. (b) Schematic of the deformation principle of the ultra-fast deformation actuator. (c) Schematic of the water transport and thermal-induced deswelling principle of the PNIPAm sponge hydrogel. (d) Schematic of the synthesis strategy of PNIPAm sponge hydrogel.

which could shorten the deformation time required for ordinary hydrogel materials from a few minutes to tens of seconds.[29] Besides, there are still some strategies to improve the porosity of hydrogels by adding porogens (such as PEG, etc.) during the polymerization process[30–32] or construct micro-scale units (such as microgels, polymer nanofibers or polymer nanosheets, etc.).[33–35] Although, a few efficient strategies have been implemented to improve the swelling/deswelling rate, the swelling/deswelling rate is still not comparable to the living organisms which could catch prey in seconds or catch the flying baseball. Therefore, it is a great challenge to achieve ultrafast actuating rate in larger sizes and change the dilemma where the existing hydrogel grippers usually only grasp stationary objects.

Herein, we have developed a hydrogel sponge actuator with ultrafast deformation rate that could grasp moving objects and living creatures (Fig. 1b, 1c). As shown in the Fig. 1d, ice, an environmentally friendly and easy-to-remove porogen, is used to construct PNIPAm hydrogels with large pores. In the presence of ice crystals, monomers are confined to specific areas and polymerized in situ to form a locally aggregated polymer network, and hydrogel sponge with micropores that are filled with water is obtained when the ice crystals melt. Due to the capillary force caused by the ice-template method, the hydrogel sponge has fast thermo-responsive swelling/deswelling rate due to the presence of capillary force. By adding a negative layer, a hydrogel sponge actuator with ultrafast deformation capability is constructed and shows application prospects in the fields of moving-objects capture and life rescue. Besides, in the practical applications, it is hard and unrealistic to transfer the hydrogel actuator to another solution with different temperature in order to trigger the thermo-responsive actuating process. Therefore, photothermal functional components are introduced into the hydrogel sponge actuator to accomplish light-controlled movement in the stable solution environment, which indicates the application and development direction of hydrogel-based soft robot with ultrafast actuating property.

2. Experimental section

2.1. Materials

N-Isopropyl acrylamide (NIPAm), acrylamide (AAm), sodium alginate (Alg), polyvinyl alcohol (PVA), ammonium persulphate (APS) were purchased from Shanghai Sinopharm Chemical Reagent Co., Ltd., *N,N′*-methylenebis (acrylamide) (BIS), *N,N,N′,N′*-tetramethylethylenediamine (TEMED), Fe_3O_4 nanoparticles were obtained from Aladdin Shanghai Reagent Co. Ltd.

2.2. Instruments

The rheological measurements were performed on a Haake MARSIII rheometer equipped with a geometry of 25 mm parallel plates at 25°C. The tensile and compression tests were performed on a CMT-1104 universal testing machine (CMT-1104, SUST Electrical Equipment Co.). The dynamic mechanical analysis was performed on a DMAQ800 analyzer (DMAQ800, TA, America). The samples were frozen in liquid nitrogen for 10 min before lyophilizing with a freeze drier (FD-1C-50, Beijing BoYiKang) at -35°C for about 48 h. The microscopic morphology was observed using a field emission scanning electron microscope (SEM, Phenon ProX) at an accelerating voltage of 10 kV. The internal pore structure was characterized using a mercury porosimeter (AutoPore IV 9500).

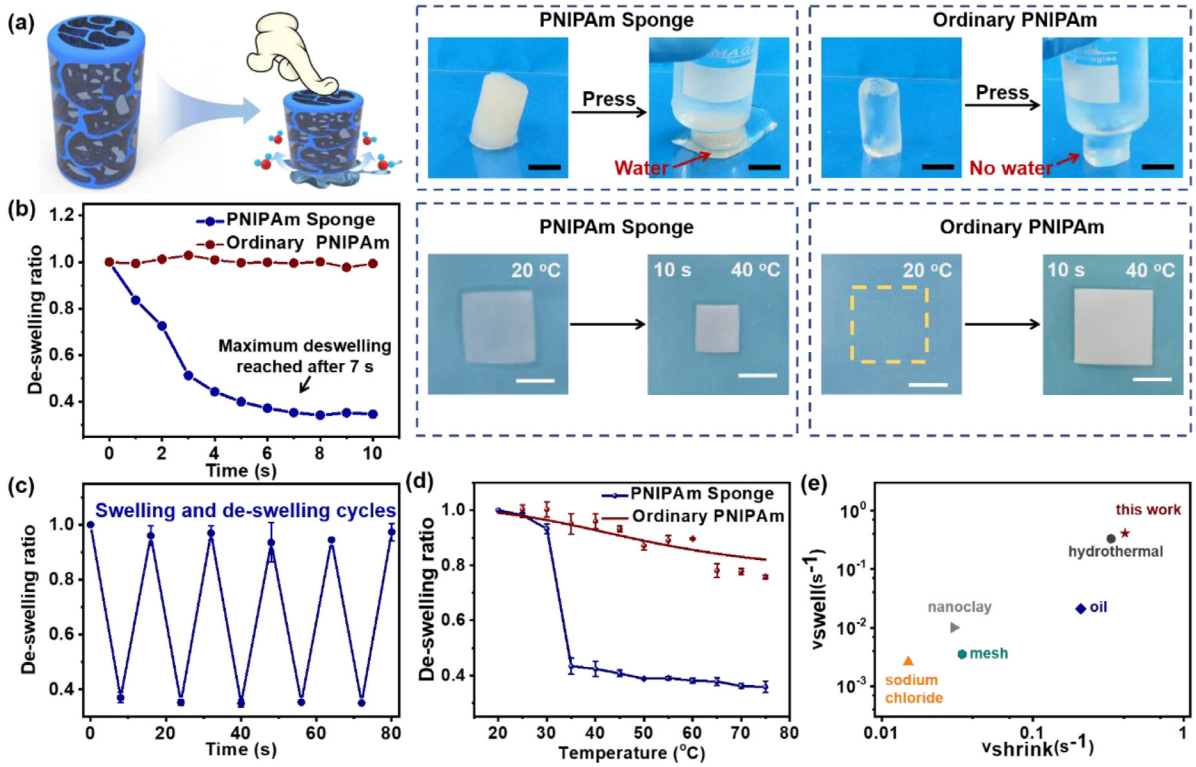

Fig. 2. (a) Digital photos of the squeezing process of PNIPAm hydrogel sponge and ordinary PNIPAm hydrogel. (b) Comparison of de-swelling rates and appearance of PNIPAm sponge hydrogel and ordinary PNIPAm hydrogel in warm water (40 °C). (c) Cyclic de-swelling and swelling performance of PNIPAm hydrogel sponge as the temperature of the water varied between 20 °C and 40 °C. (d) De-swelling ratio of PNIPAm hydrogel sponge and Ordinary PNIPAm hydrogel at different temperatures. (e) Comparison of de-swelling rate of PNIPAm hydrogel obtained by different synthesis strategies. [36–40] Scale bars: 1 cm.

2.3. Preparation of PNIPAm hydrogel sponge

NIPAm monomers (1.0 g), 10 mg of cross-linking agent Bis and 10 mg of free radical polymerization initiator APS were dissolved in 5 mL of deionized water, shaken and ultrasonicated to obtain a clear and transparent solution. After adding 10 μL of TEMED to the solution, quickly poured the above solution into a self-made mold with a thickness of 1 mm, sealed the mold with a glass sheet, and placed it in a freezer at -30 °C for 0.5 h. After the liquid was completely frozen, transfered the mold to a refrigerator at a temperature of -5 °C and polymerized for 12 h. After the polymerization, the PNIPAm hydrogel sheet was soaked in deionized water for 24 h to remove unreacted monomers.

2.4. Preparation of ordinary PNIPAm hydrogel

NIPAm monomers (1.0 g), 10 mg of cross-linking agent Bis and 10 mg of free radical polymerization initiator APS were dissolved in 5 mL of deionized water, shaken and ultrasonicated to obtain a clear and transparent solution. After adding 10 μL of TEMED to the solution, quickly poured the above solution onto a glass sheet covered with pre-moistened weighing paper, and sealed it with a 1 mm thick mold. Follow-up experiment steps are the same as above.

2.5. Preparation of bilayer PNIPAm hydrogel sponge actuator

APS (750 mg) was dissolved in 50 mL deionized water to obtain a clear solution A. AAm monomer (1.4 g), crosslinker Bis (42 mg), Fe_3O_4 nanoparticles (200 mg) and TEMED (50 μL) were dissolved in 20 mL of sodium alginate solution (2 wt%) to obtain solution B. An PNIPAm hydrogel sponge sheet with a size of 6 cm*6 cm*1 mm was soaked in 50 mL of solution A for 30 min, and placed in a mold with a thickness of 2 mm. Solution B was poured on the gel sheet and sealed with a glass sheet. The polymerization system was placed in a 4 °C environment for 1 h.

2.6. Actuation characterization

The PNIPAm hydrogel sponge actuator and ordinary PNIPAm hydrogel actuator were cut into strips of 30 mm long, 3 mm wide, and 1 mm thick, respectively, and placed in warm water at 40 °C. The change in gel bending angle was recorded by using a camera.

2.7. Finite element modeling

The force condition of the hydorgel actuators during the actuating process was analyzed and simulated by *abaqus*. The grid cell was constructed by C3D8RH:An 8-node linear brick, hybrid, constant pressure, reduced integration, hourglass control. And the modeling materials is Neo-Hookean.

3. Results and discussion

At first, the basic properties of the hydrogel sponge and ordinary hydrogel obtained using different synthetic strategies are characterized to illustrate the difference in their structures. As shown in Figure S1a, compared with the transparent ordinary PNIPAm hydrogel, the PNIPAm hydrogel sponge is almost completely opaque at room temperature. The light transmittance of them was quantitatively analyzed using an ultraviolet-visible spectrophotometer. The results are shown in Figure S1b and Figure S1c. The transmittance of PNIPAm hydrogel sponge at room temperature is almost 0, while that of ordinary PNIPAm hydrogel reaches more than 95%. The difference in transparency of these two hydrogels is closely related to the difference in the distribution of polymer networks. Specifically, in the frozen state, the squeezing effect

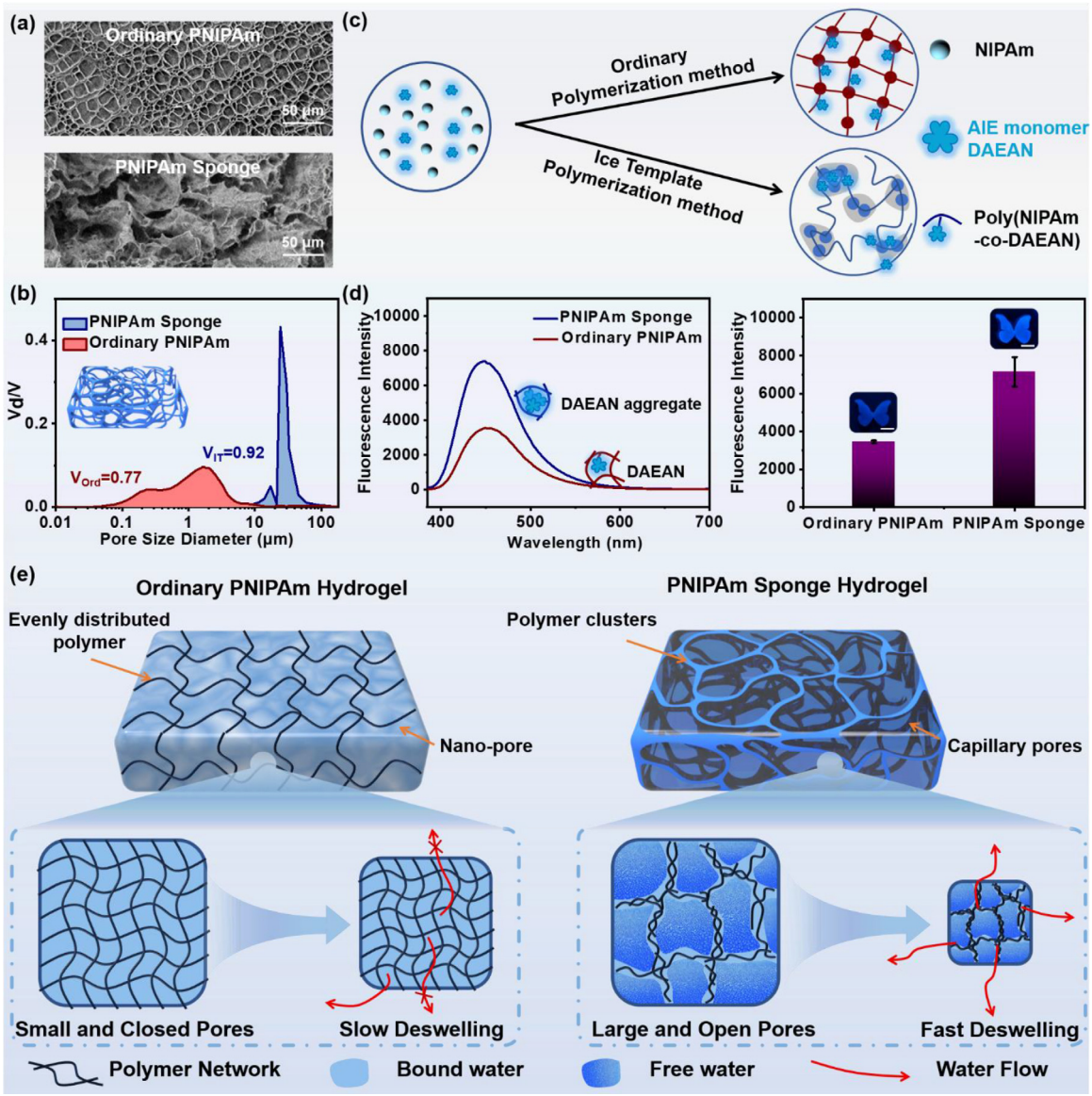

Fig. 3. (a) SEM images of the microstructure of PNIPAm hydrogel sponge and ordinary PNIPAm hydrogel. (b) Quantitative measurement of the pore structure of the PNIPAm hydrogel sponge and ordinary PNIPAm hydrogel by a mercury porosimeter. (c) Schematic of the preparation of fluorescent hydrogels synthesized by two different methods. (d) Fluorescence emission spectra of the fluorescent hydrogels synthesized by two different methods. (e) The structural model and the explanation of the rapid de-swelling mechanism of PNIPAm hydrogel sponge. Scale bars: 1 cm.

of ice crystals prevents the polymer from being evenly distributed, and the uneven structure usually results in an opaque appearance. After the polymerization reaction is completed, these squeezed polymer chains are fixed due to permanent chemical cross-linking. Moreover, PNIPAm hydrogel sponge remained opaque after being placed at 20 ˚C water for a long time after synthesis, indicating that the white appearance was not caused by the LCST effect of PNIPAm. Additionally, the water in the PNIPAm hydrogel sponge would flow out when being pressed, while no water was seen if the ordinary PNIPAm was pressed (Fig. 2a, Movie S1). The results indicate water molecules was immobilized by the PNIPAm polymer networks in the ordinary PNIPAm hydrogel, while micro channels that was filled with free water molecules presented in the PNIPAm hydrogel sponge due to the inefficient hydrogen bonding between water molecules and PNIPAm chains in the frozen state. The difference in the mechanical properties of the two hydrogel samples also provides evidence for this hypothesis. The results in Figure S2 show that the maximum tensile stress of PNIPAm hydrogel sponge is only half that of ordinary PNIPAm hydrogel.

Because of the presence of water filled micro pores, water molecules could quickly release from or fill the pores of the PNIPAm hydrogel sponge with the assistance of capillary force, the de-swelling/swelling rate of the PNIPAm hydrogel sponge is significantly enhanced. Therefore, when the two samples of PNIPAm hydrogel sponge and ordinary hydrogel were alternative immersed in 40 and 20 ˚C baths, respectively. The de-swelling rate and de-swelling ratio of the two hydrogels are significantly different. Fig. 2b depicts the time-dependent de-swelling behavior of PNIPAm hydrogel sponge and ordinary PNIPAm hydrogel. The PNIPAm hydrogel sponge exhibits a very fast de-swelling rate: the sample reaches an equilibrium state within 7 seconds, and the de-swelling ratio at this time is about 0.4. Although the ordinary PNIPAm sample quickly become opaque in 40 ˚C warm water, its volume does not change significantly after 1 minute. Fig. 2c shows that the swelling rate of hydrogel sponge is equivalent to the de-swelling rate, and the de-swelling rate of PNIPAm hydrogel sponge remains stable during the several de-swelling/swelling cycles, indicating that its micro porous structure has not been damaged in the process of cycling.

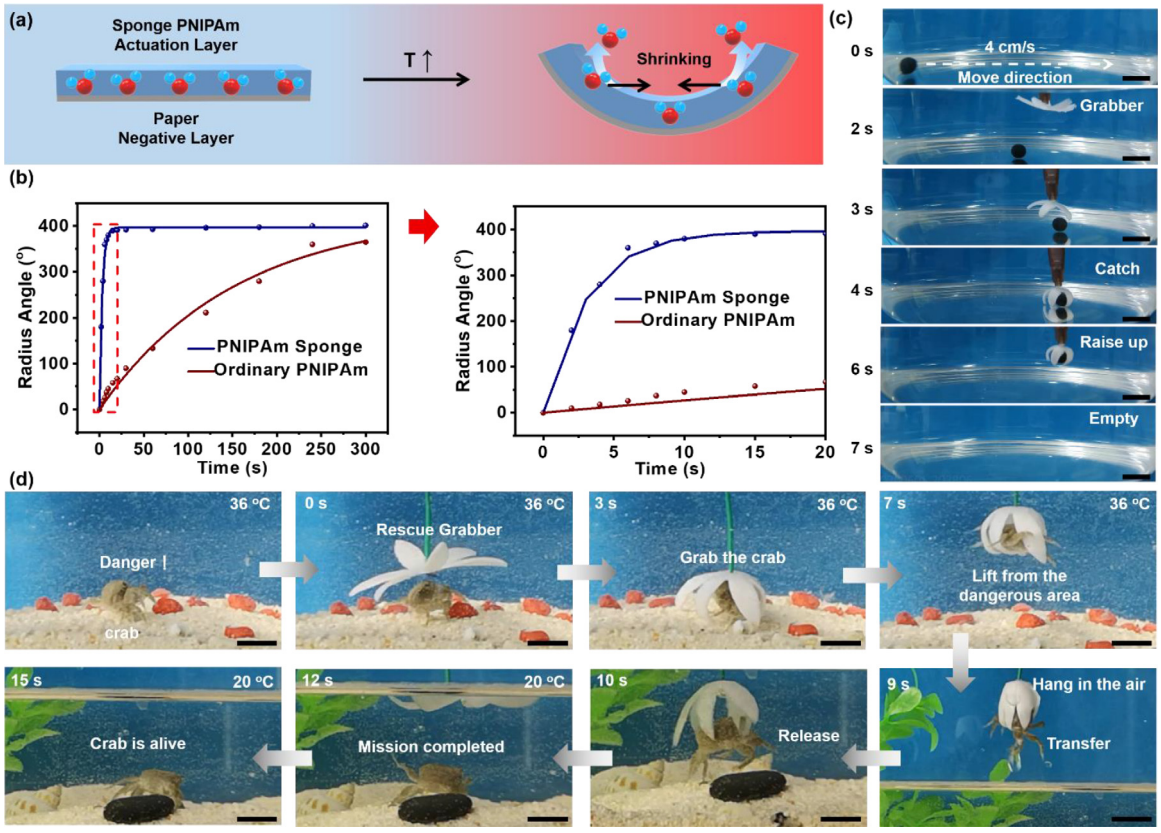

Fig. 4. (a) Schematic of the structure and bending mechanism of actuator based on PNIPAm hydrogel sponge. (b) Bending rates of actuators based on PNIPAm hydrogel sponge and ordinary PNIPAm hydrogel. (c) The ultrafast actuator based on PNIPAm hydrogel is used to grab a moving ball in water. (d) Application demonstration of ultrafast actuator based on PNIPAm hydrogel sponge: emergency rescuer. Scale bars: 1 cm.

Not only the de-swelling and swelling speed of PNIPAm hydrogel sponge is significantly faster than that of ordinary PNIPAm hydrogel, the de-swelling ratio of PNIPAm hydrogel sponge is also much smaller than that of ordinary PNIPAm hydrogel at different temperatures. As shown in Fig. 2d, below 30 °C, both hydrogel samples hardly de-swell. When the temperature reaches 35 °C, the volume of PNIPAm hydrogel sponge decreases rapidly, shrinking to about 40% of the initial volume, and the de-swelling of ordinary PNIPAm hydrogel is still not obvious. When the temperature further increased, the de-swelling ratio of PNIPAm hydrogel sponge decreased slightly with the increase of temperature. For ordinary PNIPAm hydrogels, no precipitous reduction in volume can be observed. Utilizing the difference in de-swelling ratio of the two hydrogel samples, we can "splice" the two hydrogels together to construct a composite hydrogel. Although the chemical components of the two parts are exactly the same, they will produce different deformations at the same temperature, leading to complex deformations of the entire sample and the experimental results are shown in Figure S3. The de-swelling and swelling rates were calculated by dividing the volume change rates by the swollen hydrogel volume, and compared with some representative literatures that report fast shrinking PNIPAm hydrogels. The results in Fig. 2e show that the PNIPAm hydrogel sponge in this work has excellent performance in both de-swelling rate and swelling rate. Lyophilizing tests were conducted on the fully swollen samples to calculate their solid contents, and the results are shown in Figure S4, after freeze-drying, there is no significant difference in the remaining proportions of the two gels, indicating that the difference in de-swelling performance between the two hydrogels are mainly caused by structural differences.

In order to further analyze the influence of hydrogel structure on performance, direct and indirect methods were used to characterize the microstructure of hydrogels synthesized by different strategies. Fig. 3a depicts the scanning electron microscopy (SEM) images of the two kinds of PNIPAM hydrogels. It is found that the ordinary PNIPAm sample exhibits uniform and closed pores, and the distribution is between 1-10 μm. Simultaneously, the PNIPAm sponge sample shows open pore structure with large and interpenetrating pores, it has uneven distribution and the pore size can be up to 100 μm. The difference in structure is related to the polymerization method. For the PNIPAm hydrogel sponge, it is frozen before polymerization, and the water in the hydrogel precursor froze to form large-sized ice crystals, which occupy the position of NIPAm monomers. The polymerization reaction of polymer monomers is carried out in a confined space. After the polymerization reaction is completed, the melting of ice crystals makes the spatial confinement from the outside disappear. However, the chemical crosslinks formed between the molecular chains act as new spatial confinements, making the molecular chains unable to move freely.

Furthermore, mercury porosimeter was used to quantitatively analyze the pore structure of the two hydrogels. The experimental results in Fig. 3b show that the pore size of the ordinary PNIPAm hydrogel is significantly smaller than that of the PNIPAm hydrogel sponge, which is consistent with our SEM observations above. In addition, it can be concluded that the pore volume in PNIPAm hydrogel sponge accounts for 92% of the total volume, which is much larger than 77% pore volume of Ordinary PNIPAm hydrogel. The results indicate that the polymer network in PNIPAm hydrogel sponge can only exist in a small area due to the confinement effect of ice crystals. Correspondingly, in the area where the polymer exists, the concentration of PNIPAm polymer will be much higher than the average concentration of Ordinary PNIPAm hydrogel. This conclusion can also be proved by indirect evidence. DAEAN,[41] a monomer with aggregation-induced luminescence effect (AIE) was copolymerized into the PNIPAm network by different synthesis strategies (Fig. 3c). The results in Fig. 3d show that when the concen-

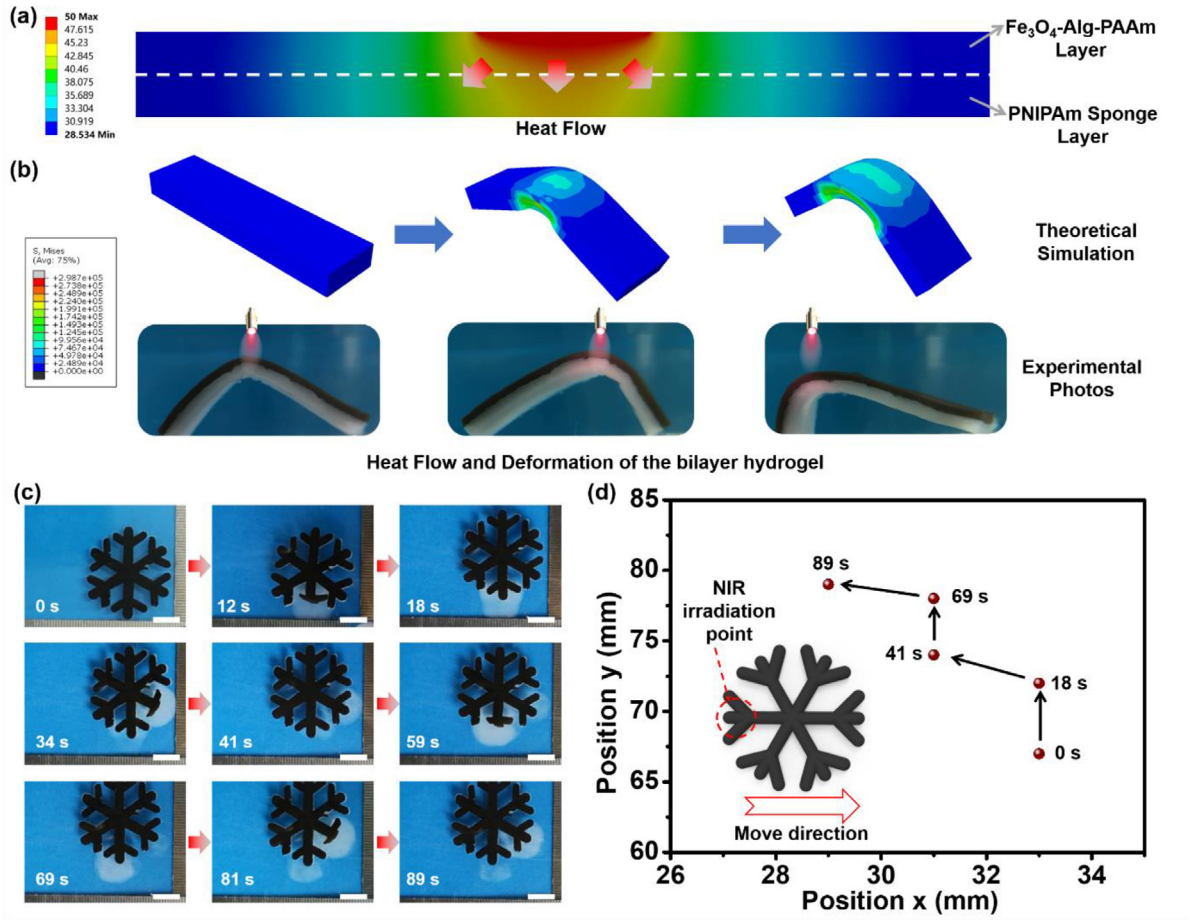

Fig. 5. (a) Calculation of heat transfer in the bilayer hydrogel. (b) Calculation results and experimental photos of local deformation of the bilayer hydrogel under local NIR light. (c) Light-controlled two-dimensional directional movement of a six-arm snow-like hydrogel on a plane. (d) The movement trajectory of the snowflake gel under the control of NIR light. Inset picture: The irradiation position and movement direction of the bilayer snowflake gel. Scale bars: 1 cm.

tration of the fluorescent components are exactly the same, the fluorescence intensity of P (NIPAm-co-DAEAN) fluorescent hydrogel sponge is more than twice that of ordinary P (NIPAm-co-DAEAN) fluorescent hydrogel, which can confirm our hypothesis on the hydrogel structure.

According to the above experimental results, it can be concluded that the hydrogel sponge structure synthesized by the ice template method has a great promotion effect on the de-swelling/swelling process of the hydrogel. This promotion effect is related to two structural characteristics of the hydrogel sponge: the polymer aggregation effect caused by the confinement of ice crystal extrusion and the capillary effect on mass transfer of large-size open pores (Fig. 3e). First, compared with ordinary PNIPAm hydrogel network with evenly distributed crosslinking points, the polymer network of PNIPAm hydrogel sponge is restricted to a smaller area, forming a large number of polymer clusters. Thus, most of the water molecules are captured in the three-dimensional networks via hydrogen bond with PNIPAm chains in ordinary PNIPAm hydrogel, while most of the water molecules (~70 %) are free distributed in the PNIPAm hydrogel sponge via capillary aisles. When thermally stimulated, the polymer clusters are less restricted and can therefore shrink quickly, in contrast, the ordinary PNIPAm hydrogel network is restricted by the tension of chemically crosslinking points and is difficult to produce significant deformation. Secondly, the capillary action would encourage the PNIPAm hydrogel sponge to squeeze out and absorb water molecules quickly, leading to the rapid de-swelling/swelling of the PNIPAm hydrogel sponge.

In some specific conditions, such as rescue, capture, and transportation, not only the soft actuator is required to be able to deform according to the required deformation procedure, but also the deformation needs to be completed in a short time. The rapid shrinkage properties of the PNIPAm hydrogel sponge encourages us to construct actuator with ultrafast deformation performance. Combining it with a temperature-insensitive pan paper, a paper-based actuator is obtained. As shown in Fig. 4a, when the hydrogel actuator is placed in warm water, the volume of the PNIPAm hydrogel sponge is reduced, while the volume of the pan paper does not change, causing the entire system to bend toward the hydrogel sponge side. Due to the rapid de-swelling of PNIPAm hydrogel sponge, the bending speed of the entire actuator is also very fast. PNIPAm hydrogel sponge and ordinary PNIPAm hydrogel were used to construct paper-based hydrogel actuators, respectively. Fig. 4b depicts the time-dependent bending behavior of paper-based actuators constructed by two different hydrogels. When placed in 40°C warm water, the PNIPAm hydrogel sponge actuator bends rapidly and reaches the final equilibrium state within 10 s and the maximum bending angle is about 400°. For ordinary PNIPAm hydrogel actuator, it takes 5 min to get the maximum bending angle of about 400°. Calculated based on the time required to reach the maximum deformation state, the deformation speed of the PNIPAm sponge-based actuator can reach more than 30 times that of ordinary PNIPAm hydrogel.

The extremely fast deformation speed of PNIPAm hydrogel sponge actuator enables it to finish some tasks that ordinary hydrogel actuator cannot do, such as capturing moving objects. Fig. 4c demonstrate the ability of the rapid-bending actuator to grab a moving ball: a small black ball moves along the bottom of a container filled with warm water at a uniform speed of 4 cm/s. When it reaches a certain position,

the grabber quickly enters the water and catches the ball. The gripping action can be completed within several seconds and then it rises from the water. The rescue of live crabs perfectly demonstrates the two major characteristics of our actuator: soft and rapid-deformation. As shown in Fig. 4d, a crab accidentally falls into warm water (36°C). Because crabs are a kind of cold-blooded animals, the temperature of experimental condition is fatal to them, it is urgent to rescue it from the high temperature environment in a short time. The PNIPAm hydrogel sponge based rapid actuator was made as "emergency rescuers". As shown in Fig. 4d, it needs only 7 seconds to grab the crab and lift it from the dangerous area. It is worth mentioning that our grabber can lift the crab from the warm water and stay in the air for several seconds, which proves the excellent gripping ability of our actuator. After transferring the crab to cold water, the grabber quickly opens and the crab is released. It can be clearly observed from the picture in Fig. 4d that the crabs in the cold water are still alive, which proves that our rescue operation is successfully completed. The rescue of multiple crabs can prove the reusability of the gripper. As shown in Figure S5 and movie S2, within 40 seconds, the thermally induced rapid deformation actuator completed 3 bending-recovery cycles, and rescued 3 crabs from the warm water, all of the crabs survived. This application provides feasible solutions for soft rescue robots and motion robots.

Additionally, the de-swelling/swelling rates can be tuned by introducing other polymers, such as polyvinyl alcohol (PVA) and sodium alginate (Alg) into PNIPAm hydrogel sponge (Figure S6a). Figure S6c-d depicts the time-dependent de-swelling behavior of PNIPAm hydrogel sponge with PVA or Alg, and the experimental results show that both PVA and Alg could reduce the de-swelling rate of the PNIPAm hydrogel sponge. The possible theoretical explanation is shown in Figure S6b, the macromolecular chains and the PNIPAm polymer network are entangled with each other, which hinders the movement of the polymer network during the thermal shrinkage of the PNIPAm network, moreover, the hydrophilic polymer chains could form interactions with water molecules, which could slow down the elimination of water molecules. In Figure S7, A series of ultrafast hydrogel actuators with different bending rates were constructed and combined to realize the multi-level deformation demonstration. When placed in warm water at 40°C, the three different petals closes one after the other. These results indicate the application potential of the PNIPAm hydrogel sponge actuator in the hierarchical deformation.

Taking advantage of the rapid deformation ability of PNIPAm hydrogel sponge, Fe_3O_4 nanoparticles with photothermal conversion ability were introduced to prepare a bilayer hydrogel actuator (Figure S8). The actuator can respond to alternating near-infrared (NIR) light stimulation to produce periodic deformation-recovery, thereby realizing directional movement of the hydrogel. The theoretical calculation in Fig. 5a shows that the heat generated by the Fe_3O_4 nanoparticles in the negative layer can be transferred to the PNIPAm hydrogel sponge layer and cause the shrinkage of the PNIPAm sponge layer. According to the calculations, when a specific part of the bilayer gel is irradiated with NIR light, the part will bend locally and the experimental results in Fig. 5b are basically consistent with the theoretical model. A serrated substrate with a specific size is designed to help the hydrogel strip move in a specific direction, as shown in Figure S9. After three alternating NIR light stimulations, the hydrogel strip moves forward 20 mm on the substrate (Figure S10 and Movie S3). Since the friction of the strip-shaped hydrogel on the ordinary smooth substrate is insufficient, the directional movement must be achieved with the help of the serrated substrate. Furthermore, in order to realize the directional movement on smooth substrate, the shape of the bilayer hydrogel must be designed. As shown in Fig. 5c, a six-armed snowflake-shaped hydrogel was constructed and placed in a square tank filled with water (Figure S11). When one side of the gel is illuminated by NIR light, it shrinks inward and pushes the hydrogel forward during the recovery process. In an on-off cycle of NIR light, the hydrogel can move 10 mm in a specific direction, and the moving direction can be tuned by irradiating different arms of the hydrogel actuator (Fig. 5d, Movie S4). Therefore, the light-controlled movement on a two-dimensional smooth substrate can be realized, which has expanded the freedom of motion of hydrogel actuator.

4. Conclusions

In this work, PNIPAm hydrogel sponge with interconnected pore structures have been fabricated. Compared with PNIPAm hydrogel that is prepared by conventional method, the PNIPAm hydrogel sponge shows large porosity and polymer aggregation due to the extrusion of ice crystal, leading to ultrafast thermally induced de-swelling/swelling properties with a de-swelling ratio of 0.4. Moreover, a bilayer hydrogel sponge actuator with rapid deformation-recovery ability have been developed, and the deformation could be completed within 10 s, which exhibits a 30 folds enhancement in actuating speed, and the ultrafast hydrogel sponge actuator could be used to grasp moving creatures. In addition, by introducing photothermal functional components and designing the shape of the hydrogel sponge, light-controlled directional movement can be realized. We believe our strategy could promote the development of soft robots with practical applications.

Conflict of interest

The authors declare no competing financial interest.

Acknowledgments

This work was supported by National Key Research and Development Program of China [2018YFB1105100], National Natural Science Foundation of China [51873223, 52073295], Key Research Program of Frontier Science, Chinese Academy of Sciences [QYZDB-SSW-SLH036].

Supplementary materials

Supplementary material associated with this article can be found, in the online version, at doi:10.1016/j.supmat.2021.100002.

References

[1] P.F. Lv, X. Lu, M. Wang L., W. Feng, Nanocellulose-based functional materials: from chiral photonics to soft actuator and energy storage, Adv. Funct. Mater. 32 (2021) NO. https://doi.org/2104991, doi:10.1002/adfm.202104991.
[2] Z. Zhao, C. Wang, H. Yan, Y. Liu, Soft robotics programmed with double crosslinking DNA hydrogels, Adv. Funct. Mater. 29 (2019), doi:10.1002/adfm.201905911.
[3] Y. Cheng, K.H. Chan, X.Q. Wang, T. Ding, T. Li, X. Lu, G.W. Ho, Direct-ink-write 3D printing of hydrogels into biome metic soft robots, ACS Nano 13 (2019) 13176–13184, doi:10.1021/acsnano.9b06144.
[4] D. Han, C. Farino, C. Yang, T. Scott, D. Browe, W. Choi, J.W. Freeman, H. Lee, Soft robotic manipulation and locomotion with a 3d printed electroactive hydrogel, ACS Appl. Mater. Interfaces 10 (2018) 17512–17518, doi:10.1021/acsami.8b04250.
[5] H. Yuk, S. Lin, C. Ma, M. Takaffoli, N.X. Fang, X. Zhao, Hydraulic hydrogel actuators and robots optically and sonically camouflaged in water, Nat. Commun. 8 (14230) (2017) NO., doi:10.1038/ncomms14230.
[6] H. Lin, S. Ma, B. Yu, X. Pei, M. Cai, Z. Zheng, F. Zhou, W. Liu, Simultaneous surface covalent bonding and radical polymerization for constructing robust soft actuators with fast underwater response, Chem. Mater. 31 (2019) 9504–9512, doi:10.1021/acs.chemmater.9b03670.
[7] P. Xue, H.K. Bisoyi, Y.H. Chen, H. Zeng, J.J. Yang, X. Yang, P.F. Lv, X.M. Zhang, A. Priimagi, L. Wang, X.H. Xu, Q. Li, Near-infrared light-driven shape-morphing of programmable anisotropic hydrogels enabled by mxene nanosheets, Angew. Chem. Int. Ed. 60 (2021) 3390–3396, doi:10.1002/anie.202014533.
[8] F. Gao, Z. Xu, Q. Liang, B. Liu, H. Li, Y. Wu, Y. Zhang, Z. Lin, M. Wu, C. Ruan, W. Liu, Direct 3D printing of high strength biohybrid gradient hydrogel scaffolds for efficient repair of osteochondral defect, Adv. Funct. Mater. 28 (1706644) (2018) NO., doi:10.1002/adfm.201706644.
[9] T. Li, J. Wang, L. Zhang, J. Yang, M. Yang, D. Zhu, X. Zhou, S. Handschuh-Wang, Y. Liu, X. Zhou, Freezing", morphing, and folding of stretchy tough hydrogels, J. Mater. Chem. B 5 (2017) 5726–5732, doi:10.1039/C7TB01265A.
[10] Q.L. Zhu, C. Du, Y. Dai, M. Daab, M. Matejdes, J. Breu, W. Hong, Q. Zheng, Z.L. Wu, Light-steered locomotion of muscle-like hydrogel by self-coordinated shape change and friction modulation, Nat. Commun. 11 (5166) (2020) NO., doi:10.1038/s41467-020-18801-1.
[11] J.C. Athas, C.P. Nguyen, B.C. Zarket, A. Gargava, Z. Nie, S.R. Raghavan, Enzyme-triggered folding of hydrogels: toward a mimic of the venus flytrap, ACS Appl. Mater. Interfaces 8 (2016) 19066–19074, doi:10.1021/acsami.6b05024.

[12] S. Xiao, Y. Yang, M. Zhong, H. Chen, Y. Zhang, J. Yang, J. Zheng, Salt-responsive bilayer hydrogels with pseudo-double-network structure actuated by polyelectrolyte and antipolyelectrolyte effects, ACS Appl. Mater. Interfaces 9 (2017) 20843–20851, doi:10.1021/acsami.7b04417.
[13] M. Guo, Y. Wu, S. Xue, Y. Xia, X. Yang, Y. Dzenis, Z. Li, W. Lei, A.T. Smith, L. Sun, A highly stretchable, ultra-tough, remarkably tolerant, and robust self-healing glycerol-hydrogel for a dual-responsive soft actuator, J. Mater. Chem. A 7 (2019) 25969–25977, doi:10.1039/C9TA10183G.
[14] Q. Zhao, X. Yang, C. Ma, D. Chen, H. Bai, T. Li, W. Yang, T. Xie, A bioinspired reversible snapping hydrogel assembly, Mater. Horiz. 3 (2016) 422–428, doi:10.1039/C6MH00167J.
[15] W. Fan, C. Shan, H. Guo, J. Sang, R. Wang, R. Zheng, K. Sui, Z. Nie, Dual-gradient enabled ultrafast biomimetic snapping of hydrogel materials, Sci. Adv. 5 (2019), doi:10.1126/sciadv.aav7174.
[16] J. Zheng, P. Xiao, X. Le, W. Lu, P. Théato, C. Ma, B. Du, J. Zhang, Y. Huang, T. Chen, Mimosa inspired bilayer hydrogel actuator functioning in multi-environments, J. Mater. Chem. C 6 (2018) 1320–1327, doi:10.1039/C7TC04879C.
[17] L. Tang, L. Wang, X. Yang, Y. Feng, Y. Li, W. Feng, Poly(*N*-isopropylacrylamide)-based smart hydrogels: design, properties and applications, Prog. Mater. Sci. 115 (2021), doi:10.1016/j.pmatsci.2020.100702.
[18] M. Cao, Y. Wang, X. Hu, H. Gong, R. Li, H. Cox, J. Zhang, T.A. Waigh, H. Xu, J.R. Lu, Reversible thermoresponsive peptide–pnipam hydrogels for controlled drug delivery, Biomacromolecules 20 (2019) 3601–3610, doi:10.1021/acs.biomac.9b01009.
[19] Y.S. Zhao, C. Xuan, X.S. Qian, Y. Alsaid, M. Hua, L.H. Jin, X. He, Soft phototactic swimmer based on self-sustained hydrogel oscillator, Sci. Robot. 4 (2019), doi:10.1126/scirobotics.aax7112.
[20] W.J. Zheng, N. An, J.H. Yang, J. Zhou, Y.M. Chen, Tough al-alginate/poly(*N*-isopropylacrylamide) hydrogel with tunable LCST for soft robotics, ACS Appl. Mater. Interfaces 7 (2015) 1758–1764, doi:10.1021/am507339r.
[21] E. Zhang, T. Wang, W. Hong, W. Sun, X. Liu, Z. Tong, Infrared-driving actuation based on bilayer graphene oxide-poly(*N*-isopropylacrylamide) nanocomposite hydrogels, J. Mater. Chem. A 2 (2014) 15633–15639, doi:10.1039/C4TA02866J.
[22] S. Xiao, M. Zhang, X. He, L. Huang, Y. Zhang, B. Ren, M. Zhong, Y. Chang, J. Yang, J. Zheng, Dual salt- and thermoresponsive programmable bilayer hydrogel actuators with pseudo-interpenetrating double-network structures, ACS Appl. Mater. Interfaces 10 (2018) 21642–21653, doi:10.1021/acsami.8b06169.
[23] Z. Liu, Y. Faraj, X.J. Ju, W. Wang, R. Xie, L.Y. Chu, Nanocomposite smart hydrogels with improved responsiveness and mechanical properties: a mini review, J. Polym. Sci. Pol. Phys. 56 (2018) 1306–1313, doi:10.1002/polb.24723.
[24] W.W. Thein-Han, R.D. Misra, Biomimetic chitosan–nanohydroxyapatite composite scaffolds for bone tissue engineering, Acta Biomater. 5 (2009) 1182–1197, doi:10.1016/j.actbio.2008.11.025.
[25] S. Jiang, F. Liu, A. Lerch, L. Ionov, S. Agarwal, Unusual and superfast temperature-triggered actuators, Adv. Mater. 27 (2015) 4865–4870, doi:10.1002/adma.201502133.
[26] S. Chang, M. Kim, S. Oh, J.H. Min, D. Kang, C. Han, T. Ahn, W.G. Koh, H. Lee, Multi-scale characterization of surface-crosslinked superabsorbent polymer hydrogel spheres, Polymer 145 (2018) 174–183, doi:10.1016/j.polymer.2018.04.073.
[27] C. Ji, A. Khademhosseini, F. Dehghani, Enhancing cell penetration and proliferation in chitosan hydrogels for tissue engineering applications, Biomaterials 32 (2011) 9719–9729, doi:10.1016/j.biomaterials.2011.09.003.
[28] T. Gancheva, N. Virgilio, Enhancing and tuning the response of environmentally sensitive hydrogels with embedded and interconnected pore networks, Macromolecules 49 (2016) 5866–5876, doi:10.1021/acs.macromol.6b01411.
[29] H. Guo, J. Cheng, J. Wang, P. Huang, Y. Liu, Z. Jia, X. Chen, K. Sui, T. Li, Z. Nie, Reprogrammable ultra-fast shape-transformation of macroporous composite hydrogel sheets, J. Mater. Chem. B 5 (2017) 2883–2887, doi:10.1039/C6TB02198K.
[30] A.E. Coukouma, S.A. Asher, Increased volume responsiveness of macroporous hydrogels, *Sensor. Actuat. B-Chem.* 255 (2018) 2900–2903, doi:10.1016/j.snb.2017.09.109.
[31] R. Sato, R. Noma, H. Tokuyama, Preparation of macroporous poly(*N*-isopropylacrylamide) hydrogels using a suspension–gelation method, Eur. Polym. J. 66 (2015) 91–97, doi:10.1016/j.eurpolymj.2015.01.051.
[32] T. Zhang, Z. Xu, H. Gui, Q. Guo, Emulsion-templated, macroporous hydrogels for enhancing water efficiency in fighting fires, J. Mater. Chem. A 5 (2017) 10161–10164, doi:10.1039/C7TA02319G.
[33] Y. Liu, K. Zhang, J. Ma, G.J. Vancso, Thermoresponsive semi-IPN hydrogel microfibers from continuous fluidic processing with high elasticity and fast actuation, ACS Appl. Mater. Interfaces 9 (2017) 901–908, doi:10.1021/acsami.6b13097.
[34] Y. Yang, Y. Tan, X. Wang, W. An, S. Xu, W. Liao, Y. Wang, Photothermal nanocomposite hydrogel actuator with electric-field-induced gradient and oriented structure, ACS Appl. Mater. Interfaces 10 (2018) 7688–7692, doi:10.1021/acsami.7b17907.
[35] Y. Zheng, Y. Cheng, J. Chen, J. Ding, M. Li, C. Li, J.C. Wang, X. Chen, Injectable hydrogel-microsphere construct with sequential degradation for locally synergistic chemotherapy, ACS Appl. Mater. Interfaces 9 (2017) 3487–3496, doi:10.1021/acsami.6b15245.
[36] R.C. Luo, J. Wu, N.D. Dinh, C.H. Chen, Gradient porous elastic hydrogels with shape-memory property and anisotropic responses for programmable locomotion, Adv. Funct. Mater. 25 (2015) 7272–7279, doi:10.1002/adfm.201503434.
[37] H. Tokuyama, Kanehara, A. Novel synthesis of macroporous poly(*N*-isopropylacrylamide) hydrogels using oil-in-water emulsions, Langmuir 23 (2007) 11246–11251, doi:10.1021/la701492u.
[38] S.X. Cheng, J.Y. Zhang, R.X. Zhuo, Macroporous poly(*N*-isopropylacrylamide) hydrogels with fast response rates and improved protein release properties, J. Biomed. Mater. Res. Part A 67A (2003) 96–103, doi:10.1002/jbm.a.10062.
[39] C. Yao, Z. Liu, C. Yang, W. Wang, X.J. Ju, R. Xie, L.Y. Chu, Poly(*N*-isopropylacrylamide)-clay nanocomposite hydrogels with responsive bending property as temperature-controlled manipulators, Adv. Funct. Mater. 25 (2015) 2980–2991, doi:10.1002/adfm.201500420.
[40] C. Yu, Z. Duan, P. Yuan, Y. Li, Y. Su, X. Zhang, Y. Pan, L.L. Dai, R.G. Nuzzo, Y. Huang, H. Jiang, J.A. Rogers, Electronically programmable, reversible shape change in two- and three-dimensional hydrogel structures, Adv. Mater. 25 (2013) 1541–1546, doi:10.1002/adma.201204180.
[41] H.Y. Qiu, S.X. Wei, H. Liu, B.B. Zhan, H.Z. Yan, W. Lu, J.W. Zhang, S. Wu, T. Chen, Programming multistate aggregation-induced emissive polymeric hydrogel into 3D structures for on-demand information decryption and transmission, Adv. Intell. Syst. 3 (2000239) (2021) NO. 2000239, doi:10.1002/aisy.202000239.